Are differential diffusion effects of importance when burning hydrogen under elevated pressures and temperatures?

Citation for the original published paper (version of record):
Mousavi, S., Lipatnikov, A. (2024). Are differential diffusion effects of importance when burning hydrogen under elevated pressures
and temperatures?. International Journal of Hydrogen Energy, 49(B): 1048-1058.
http://dx.doi.org/10.1016/j.ijhydene.2023.10.050

Available online at www.sciencedirect.com

ScienceDirect

journal homepage: www.elsevier.com/locate/he

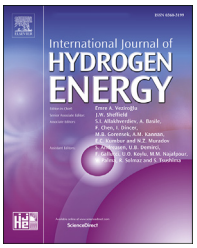

Are differential diffusion effects of importance when burning hydrogen under elevated pressures and temperatures?

Seyed Morteza Mousavi, Andrei N. Lipatnikov *

Department of Mechanics and Maritime Sciences, Chalmers University of Technology, Gothenburg SE-412 96, Sweden

HIGHLIGHTS

- Magnitude of differential diffusion effects is increased by pressure.
- Magnitude of such effects is decreased with increasing temperature.
- These trends are controlled by variations in Zel'dovich number.
- Differential diffusion effects are of importance under engine conditions.

ARTICLE INFO

Article history:
Received 11 May 2023
Received in revised form
16 August 2023
Accepted 4 October 2023
Available online xxx

Keywords:
Differential diffusion
Lewis number
Strained flames
Consumption velocity
Elevated pressure
Elevated temperature

ABSTRACT

A ratio of turbulent burning velocity to laminar flame speed is well known to be abnormally high in lean hydrogen-air mixtures, with this phenomenon being commonly attributed to differential diffusion effects. Magnitude of such effects is known to be increased by pressure, but a few recent studies have indicated that the effects are mitigated when reactants are preheated. It is not yet known, however, which of these two counteracting trends is of more importance under elevated pressures and temperatures associated with combustion in engines. Accordingly, it is not yet clear whether or not models of differential diffusion effects are required for research and development of future ultra-clean and highly efficient engines that burn hydrogen (the emphasized effects are typically ignored in engineering computations). To clarify the issue, numerical simulations of lean complex-chemistry hydrogen-air strained laminar flames are performed by varying strain rate, pressure $1 \leq P \leq 50$ bar, temperature $300 \leq T_u \leq 900$ K, and equivalence ratio ($\Phi = 0.4$, 0.55, and 0.7). This simple problem is selected because maximal consumption speeds reached in critically strained (close to extinction) lean hydrogen-air laminar flames are considered to characterize the influence of differential diffusion on turbulent burning rates within the framework of Zel'dovich's leading point concept, which was well supported in recent studies. Computed results show that, even at $T_u = 900$ K, the aforementioned consumption speeds are significantly larger than the unperturbed laminar flame speeds if the mixture is sufficiently lean (the equivalence ratio $\Phi = 0.55$ or lower) and pressure is sufficiently high ($P \geq 30$ bar). Therefore, differential diffusion effects are expected to be of importance when burning so lean hydrogen-air mixtures in engines and should be properly modeled.

* *Corresponding author.*
E-mail address: lipatn@chalmers.se (A.N. Lipatnikov).

https://doi.org/10.1016/j.ijhydene.2023.10.050

1. Introduction

Over the past decade, interest in hydrogen combustion has rapidly been growing [1–20], because the threat of global warming calls urgently for sustainable transition from consumption of energy bound in fossil fuels to efficient utilization of renewable, carbon-free energy sources. Accordingly, hydrogen is widely recognized to be a promising alternative energy carrier capable for replacing fossil fuels in various engines [21–29]. Expansion of hydrogen in energy production and transportation sectors could substantially be accelerated by advancing various tools for R&D of future highly efficient and ultra-clean technologies for burning H_2. Such tools include, in particular, Computational Fluid Dynamics (CFD) software. Yet, to be a valuable R&D tool, a CFD package should be not only user-friendly and numerically efficient, but also predictive or, in other words, should involve high fidelity, physics-based models of the most important relevant phenomena. From the latter perspective, however, the utility of CFD tools for research into turbulent burning of hydrogen is strongly limited by inability of a typical model of flame-turbulence interaction, implemented into a modern CFD software, to predict abnormally high ratios of turbulent burning velocity U_T and laminar flame speed S_L.

As reviewed elsewhere [30–32], this phenomenon is well documented by numerous research groups in various experiments with lean H_2-containing mixtures, see also Refs. [33–46], and in recent Direct Numerical Simulation (DNS) studies of lean hydrogen-air turbulent flames [47–52]. For instance, experimental data by Karpov and Severin [34] showed $U_T/S_L = 1.44$ and 8.3 in rich (the equivalence ratio $\Phi = 5.0$) and lean ($\Phi = 0.18$) hydrogen-air mixtures under the same turbulence conditions, i.e., the normalized turbulent burning velocities differed by a factor of about six. Recently, Yang et al. [42] reported normalized turbulent flame speed S_T/S_L as large as 130 000 in a very lean $H_2/O_2/CO_2$ mixture, see Fig. 4 in the cited paper, whereas S_T/S_L obtained from a rich $H_2/O_2/CO_2$ mixture in those experiments was slightly above unity.

The phenomenon is widely accepted to result from high molecular diffusivity of H_2 or, more specifically, from local variations in temperature, mixture composition, and reaction rates due to imbalance of molecular fluxes of fuel and heat to and from, respectively, reaction zones stretched by turbulent eddies [30–32]. For instance, recent DNS data [49] show that suppression of such differential diffusion effects by setting molecular diffusivities of all species equal to molecular heat diffusivity of the mixture results in decreasing U_T/S_L by a factor of about five in a lean ($\Phi = 0.35$) hydrogen-air mixture. While this governing physical mechanism (differential diffusion) yielding the abnormally high ratios of U_T/S_L is known, it is not yet properly addressed by the vast majority of premixed turbulent combustion models and, in particular, by models implemented into state-of-the-art CFD software. This limitation significantly reduces the utility of CFD tools for R&D of engines that burn hydrogen.

Nevertheless, as far as hydrogen-fueled engines are concerned, importance of the discussed differential diffusion effects could be put into question, because combustion in an engine occurs under elevated pressures and temperatures. On the one hand, results of experimental [40,46] and three-dimensional DNS [51,53] studies show that an increase in U_T/S_L due to differential diffusion effects is enhanced by pressure if $1 \le P \le 10$ atm. Recent two-dimensional DNSs [53] performed at $P = 20$ atm and three-dimensional DNSs [52] performed at $1 \le P \le 40$ bar support this trend also. Moreover, two-dimensional simulations [53,54] of lean hydrogen-air laminar flames, which are unstable due to differential diffusion effects [55–57], also indicate that such effects are more pronounced at higher pressures. Thus, an increase in P was shown [40,46,51–54] to be beneficial for differential diffusion effects both in laminar and turbulent flames. However, pressures explored in the cited papers, with the exception of Ref. [52], are significantly less than a typical pressure in, e.g., a piston engine.

On the other hand, an increase in unburned gas temperature T_u appears to act in the opposite direction. Indeed, first, results of two-dimensional simulations of lean hydrogen-air laminar flames [54] show that their thermo-diffusion instability is mitigated when preheating the mixture. Second, DNS data [53] obtained from lean ($\Phi = 0.3$) H_2-air turbulent flames indicate that differential diffusion effects are not pronounced at $T_u = 750$ K and $P = 1$ atm. Thus, an increase in T_u could reduce differential diffusion effects both in laminar and turbulent lean hydrogen-air flames, see Ref. [52] also.

This recently found trend [52–54] raises a question of whether or not differential diffusion effects play an important role in lean hydrogen-air flames under elevated temperatures and pressures associated with combustion in engines. In other words, whether or not reduction of differential-diffusion-effect magnitude due to an increase in T_u overwhelm an increase in the effect magnitude by P under engine conditions. The present work aims at numerically exploring this issue.

The adopted method and simulation setup are discussed in the next section. Numerical results are presented and analyzed in the third section followed by conclusions.

2. Methodology

2.1. Problem statement

Since a target-directed study of differential diffusion effects in lean complex-chemistry hydrogen-air three-dimensional turbulent flames in a wide range of elevated pressures and elevated temperatures does not seem to be feasible, an indirect method is adopted in this work based on the following two reasons.

First, the present authors are aware on only two numerical studies [58,59], where high ratios of U_T/S_L measured in lean turbulent flames fueled with H_2 were quantitatively predicted, with both studies being based on a leading point concept. As reviewed elsewhere [30–32], this concept was developed by Zel'dovich and other experts from the Russian school. The concept is based on a hypothesis that propagation of a premixed turbulent flame is controlled by its elements that advance furthest into unburned gas (so-called leading points). Besides this simple hypothesis, the concept is also based on the mathematical theory of convection-diffusion-reaction (CDR) equations. Such equations are widely used in various

Please cite this article as: Mousavi SM, Lipatnikov AN, Are differential diffusion effects of importance when burning hydrogen under elevated pressures and temperatures?, International Journal of Hydrogen Energy, https://doi.org/10.1016/j.ijhydene.2023.10.050

fields of modern science [60,61], while mathematical analysis of this class of partial differential equations was pioneered by studying biological problems [62–65]. In particular, the seminal KPP theorem proved rigorously by Kolmogorov, Petrovsky, and Piskounov [63] for a wide subclass of CDR equations highlights the crucial role played by the leading edge of a travelling wave in its propagation. In the combustion literature, the KPP theory was adapted for modeling turbulent premixed flames [66–74]. Moreover, the theory yields mathematical foundations for the leading point concept, which was further supported in recent experimental [39,40,75], theoretical [76–79], and DNS [49,52,80–84] studies.

Second, within the framework of this concept, turbulent burning velocity is hypothesized to be controlled by local characteristics of critically perturbed, inherently laminar reaction zones localized to the leading edge of a turbulent flame brush [30–32]. In a turbulent flow, reaction zones are perturbed due to their curvature and due to strain rates created by turbulent eddies, with both highly curved [31,58] and highly strained [30,85] laminar flames being proposed to be used as simple models of the local structure of leading reaction zones. Recently, the latter hypothesis was quantitatively supported in Reynolds-Averaged Navier-Stokes [59] and direct numerical [83,86] simulations of turbulent combustion. In particular, an analysis [86] of DNS data obtained from seven different complex-chemistry hydrogen-air flames, characterized by different equivalence ratios, different r.m.s. turbulent velocities u', and different integral length scales L, has shown that the peak (over the entire computational domain) local fuel consumption rates (i) are almost always (at various instants) detected in the vicinity of the flame-brush leading edges and (ii) are close to fuel consumption rates obtained from the counterpart critically strained laminar flames. Henceforth, term "strained laminar flames" refers to twin, planar, one-dimensional laminar premixed flames stabilized in reactant counterflows, see Fig. 1b in the next section. Note that, in the studied lean hydrogen-air mixtures, these two fuel consumption rates are significantly (by a factor of 16 [86]) higher than the fuel consumption rate in the counterpart unperturbed (planar, one-dimensional, and fully developed) laminar premixed flame. These recent findings highlight the aforementioned critically strained laminar premixed flame as an appropriate simple model of the local structure of leading reaction zones in turbulent flows. Utility of local burning rates obtained from such laminar flames for predicting turbulent burning velocities was also demonstrated by analyzing experimental data [39,40,75] obtained from lean H_2-containing mixtures.

Jointly with the leading point concept, these recent findings imply that turbulent flame propagation is controlled by highly strained, inherently laminar leading reaction zones whose local characteristics are affected by eventual imbalance of molecular fluxes of fuel and heat to and from, respectively, these zones. Specifically, in a lean hydrogen-air mixture, molecular flux of H_2 into highly strained reaction zones overwhelms heat losses from them, with the local temperature and burning rate being significantly increased when compared to the unperturbed laminar flame. Within the framework of the outlined physical scenario [30], abnormally high ratios of U_T/S_L, well documented in such mixtures [31,32,42], can be computed (in the first approximation) by substituting fuel consumption rates obtained from unperturbed laminar flames with fuel consumption rates obtained from the counterpart critically strained laminar flames [59]. In other words, while a number of physical scenarios of local flame-turbulence interactions can be realized within a premixed turbulent flame brush, solely highly strained, thin, inherently laminar reaction zones localized to the leading edge of the flame brush are in the focus of the leading point concept. Accordingly, the influence of differential diffusion phenomena on turbulent burning velocity can be explored by computing local burning rate in highly strained laminar premixed flames. The present authors are not aware on another approach whose capabilities for predicting a strong increase in U_T/S_L due to differential diffusion effects in lean H_2-air mixtures are documented. Based on all these reasoning, a specific goal of the present study consists in exploring the influence of elevated temperatures and pressures on the highlighted burning rate obtained numerically from strained complex-chemistry laminar premixed flames.

Finally, the following issue should be borne in mind. Such simulations require detailed chemical mechanisms of hydrogen burning, but capabilities of available mechanisms for predicting laminar flame speeds under elevated pressures

Fig. 1 – Sketches of (a) unperturbed laminar flame and (b) twin strained flames stabilized in reactant counterflows.

Please cite this article as: Mousavi SM, Lipatnikov AN, Are differential diffusion effects of importance when burning hydrogen under elevated pressures and temperatures?, International Journal of Hydrogen Energy, https://doi.org/10.1016/j.ijhydene.2023.10.050

and temperatures have not yet been validated, because measurements of S_L in lean H_2/air mixtures are extremely difficult under such conditions. From this perspective, results reported in the following may be put into question. Nevertheless, the present authors are not aware on a better tool for evaluating speeds of lean H_2/air laminar flames under elevated pressures and temperatures, with complex-chemistry simulations being widely used for this purpose by the engine and combustion communities. Therefore, research method adopted in this work is consistent with the state of the art. Besides, to address concern regarding predictive capabilities of selected chemical mechanisms, three different state-of-the-art mechanisms were used, as discussed in the next subsection.

2.2. *Numerical simulations of unperturbed and strained laminar flames*

Numerical results reported in the next section were obtained by simulating unperturbed, see Fig. 1a, or strained, see Fig. 1b, lean hydrogen-air laminar flames. Both flames are adiabatic and are described by the ideal gas state equation and stationary, one-dimensional standard transport equations for mass, momentum, species concentrations, and energy. In the former case, the reactant flow is uniform and one-dimensional. In the latter case, the reactant flow is non-uniform and two-dimensional, i.e., $\mathbf{u} = \{u(x), v(r)\}$ with $du/dx < 0$, but the problem is still described with one-dimensional transport equations [87], because all mixture characteristics are independent of r near the symmetry axis, with the radial pressure gradient $\partial p/\partial r \propto r$. Molecular mass transfer and molecular heat transfer are described by multi-component transport model, which yields different diffusivities for different pressures. Soret effect is also considered. Combustion chemistry is modeled using three state-of-the-art detailed chemical mechanisms [88–90], which gave the same answer to the question posed in the paper title. For brevity, only results obtained using the mechanism by Burke et al. [88] are reported in the following, with the exception of Fig. 6, where results computed adopting all the three mechanisms [88–90] are compared. Three equivalence ratios, i.e., $\Phi = 0.4$, 0.55, and 0.7, are addressed in the present work. Unburned gas temperatures and pressures are varied in the following ranges: 300 K $\leq T_u \leq$ 900 K and 1 atm $\leq P \leq$ 50 bar, respectively. So high unburned gas temperature was used to study conditions that are least favorable for differential diffusion effects.

All simulations were run using the open-source software toolkit Cantera [91]. In the considered cases, governing partial differential equations degenerate to a set of non-linear ordinary differential equations, which were iteratively solved. The numerical grid was automatically refined when a normalized slope or curvature of computed variables exceeded 0.01 at any point. In the case of twin strained flames, see Fig. 1b, only one of them was simulated and symmetry conditions were set at the symmetry boundary. The computational domain width was typically equal to 10 mm but was reduced to 1 mm at high temperatures or pressures to achieve better numerical stability.

The major task of the present simulations consists in evaluating displacement, S_d, and consumption, S_c, speeds in strained laminar flames using the module "CounterflowTwinPremixedFlame" in Cantera [91]. Following common practice, S_d is equal to the minimum axial flow velocity $u(x)$ upstream of the flame, see Fig. 2a. The consumption speed is evaluated as follows:

$$S_c = \frac{1}{\rho_u (T_b - T_u)} \int_{-\infty}^{0} \frac{\dot{q}}{c_p} dx, \tag{1}$$

Here, $\dot{q}$ designates heat release rate; c_p is heat capacity of the mixture at constant pressure; subscripts u and b refer to unburned reactants and adiabatic equilibrium combustion products, respectively. The strain rate κ is associated with the most negative value of the velocity gradient du/dx, i.e., $\kappa = |\min\{du/dx\}|$, which is also reached upstream of the reaction zone, see Fig. 2b. The increasing branches of curves plotted in Fig. 2 result from thermal expansion in the flame. For each set $\{\Phi, P, T_u\}$ of conditions, dependencies of $S_c(\kappa)$ and $S_d(\kappa)$ were computed by gradually increasing the inlet flow velocity U_g until the flame was quenched.

Moreover, simulations of unperturbed laminar flames were performed using the "FreeFlame" module in Cantera [91]. Those simulations aimed at evaluating flame characteristics

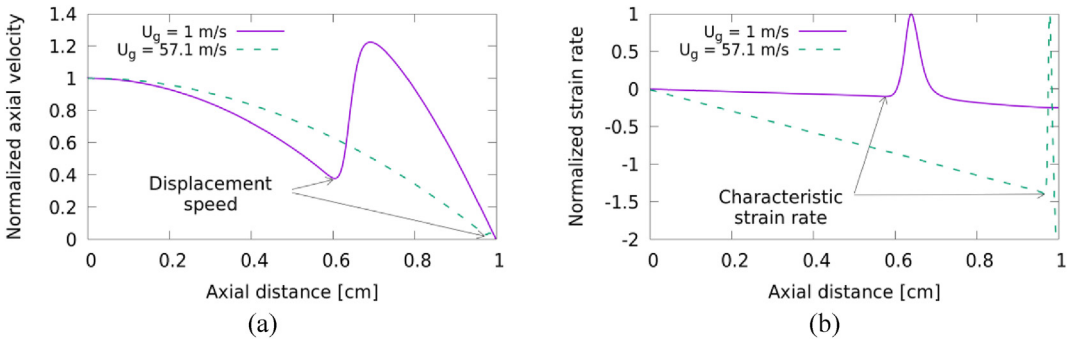

Fig. 2 – Evaluation of (a) displacement speed S_d and (b) strain rate κ by processing dependencies of the axial velocity $u(x)$ and its axial derivative du/dx, respectively, on the axial distance x counted from the nozzle exit ($x = 1$ cm at the symmetry axis). Results obtained from a weakly strained flame and a critically strained flame are plotted in solid and dashed lines, respectively, with U_g designating the inlet axial velocity. Displacement speed is normalized using S_L and du/dx is normalized using its maximal positive value, which is equal to (a) 2.1 1/ms or (b) 8.2 1/ms. $\Phi = 0.4$, $P = 1$ bar, $T_u = 300$ K.

Please cite this article as: Mousavi SM, Lipatnikov AN, Are differential diffusion effects of importance when burning hydrogen under elevated pressures and temperatures?, International Journal of Hydrogen Energy, https://doi.org/10.1016/j.ijhydene.2023.10.050

required to explain dependencies of $S_c(\kappa,\Phi,P,T_u)$ and $S_d(\kappa,\Phi,P,T_u)$ obtained from the strained flames. Computed for these purposes are (i) unperturbed laminar flame speeds $S_L(\Phi,P,T_u)=S_c(\Phi,P,T_u)$ with respect to reactants; (ii) adiabatic combustion temperatures $T_b(\Phi,P,T_u)$; (iii) dependencies of fuel consumption rate $\dot{\omega}_F(c_F,\Phi,P,T_u)$ and heat release rate $\dot{q}(c_T,\Phi,P,T_u)$ on fuel-based and temperature-based combustion progress variables, $c_F=1-X_{H_2}/X_{H_2,u}$ and $c_T=(T-T_u)/(T_b-T_u)$, respectively; (iv) activation temperatures $T_a(\Phi,P,T_u)$; and (v) Zel'dovich numbers $Ze(\Phi,P,T_u)\equiv T_a(T_b-T_u)/T_b^2$. Here, X_{H_2} designates mole fraction of H_2 and the activation temperatures are evaluated following a widely used method proposed by Law and Sung [92].

Specifically, (i) dependencies of the mass burning rates $f=\rho_u S_L$ on T_b are obtained for a set of flames, where N_2 is partially substituted with Ar (up to 20 % moles of N_2); and the activation temperature is calculated as follows

$$T_a=2T_b^2\frac{d\left[\ln\left(f/f^{ref}\right)\right]}{dT_b}, \tag{2}$$

where superscript *ref* is used for reference conditions. Equation (2) reads

$$T_a=-2\frac{d\left[\ln\left(f/f^{ref}\right)\right]}{d(1/T_b)}, \tag{3}$$

thus, demonstrating that the activation temperature is equal to the slope of a curve, which shows dependence of $2\ln(f/f^{ref})$ on $1/T_b$. A typical example of such a linear dependence is plotted in Fig. 3.

3. Results and discussion

Typical computed dependencies of normalized displacement, S_d/S_L, and consumption, S_c/S_L, speeds on normalized strain rate, $\chi\tau_f\kappa$, are reported in dashed and solid lines, respectively, in Fig. 4. Here, the time scale $\tau_f=D_{H_2,u}/S_L^2$ characterizes unperturbed laminar premixed flames; $D_{H_2,u}$ is molecular diffusivity of hydrogen in unburned reactants; in order for the abscissa coordinates of the most right edges of the computed curves to be comparable under different conditions in each subfigure, the strain rate is normalized using the factor χ specified in subfigure captions; $P^*=1$ bar and $T_u^*=300$ K are reference pressure and temperature, respectively. The critical strain rates were found by gradually increasing the inlet flow velocity U_g and, hence, κ until the flame was quenched by a too high strain rate. Subsequently, the highest value of κ that the flame survived was considered to be the critical strain rate under each set $\{\Phi,P,T_u\}$ of conditions. Therefore, the critical strain rates are associated with the most right edges of the computed curves.

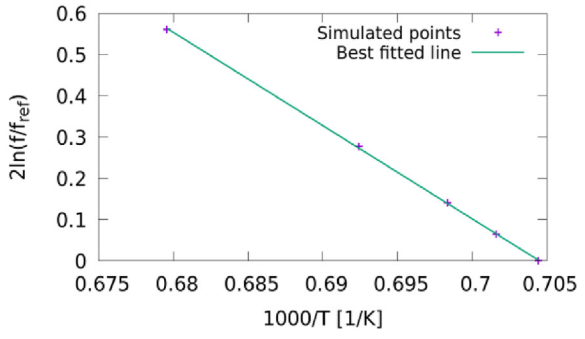

Fig. 3 – A typical dependence of $2\ln(f/f^{ref})$ on the inverse adiabatic combustion temperature $1000/T_b$, computed by partially substituting N_2 with Ar. The slope of the linear fit (line) to the computed data (symbols) is equal to the activation temperature. $\Phi=0.4$, $P=1$ bar, $T_u=300$ K.

The following trends observed in Fig. 4 are worth emphasizing. First, Fig. 4a, c, and 4d show that both S_d/S_L and S_c/S_L are increased by the flame strain rate in the studied lean hydrogen-air mixtures ($\Phi=0.55$ or 0.40), with the former ratio being larger. Such trends are well known and are commonly attributed to differential diffusion effects [30–32,39,40,43,46,47,59,83,86]. Second, both S_d/S_L and S_c/S_L are increased by pressure, see Fig. 4a, in line with earlier studies [40,46,51,53,54], which have indicated that differential diffusion effects are more pronounced at higher pressures. Third, critical strain rates are also higher at higher P, see Fig. 4a and note that $\chi\ll1$ at $P=25$ or 50 bar. On the contrary, fourth, both S_d/S_L and S_c/S_L are decreased with increasing T_u, see Fig. 4b, in line with earlier studies [53,54], which have indicated that differential diffusion effects are less pronounced at higher temperatures. In particular, S_d/S_L is close to unity and S_c/S_L is less than unity in highly preheated strained flames characterized by $\Phi=0.55$ and $P=1$ bar, see blue lines with stars in Fig. 4b. Fifth, critical strain rates are also lower at higher T_u, see Fig. 4b and note that $\chi\gg1$ at $T_u=600$ or 900 K. Nevertheless, sixth, if not only T_u, but also P are increased, S_d/S_L, S_c/S_L, and the critical $\tau_f\kappa$ are higher at elevated pressures and temperatures, see Fig. 4c, where $\chi=1$. Seventh, a decrease in the equivalence ratio results in significantly increasing S_d/S_L, S_c/S_L, and the critical $\tau_f\kappa$, cf. axis scales in Fig. 4c and d, which show results computed at $\Phi=0.55$ and 0.4, respectively.

Fig. 4c and d indicate that reduction of differential diffusion effect magnitude due to an increase in T_u does not overwhelm (under conditions of the present simulations) an increase in the effect magnitude by P, i.e., the discussed effects are expected to be of importance even at the highest T_u and P addressed in the present study. The same trend is shown in Fig. 5, which reports dependencies of the peak normalized consumption speed $\max\{S_c(\tau_f\kappa)\}/S_L$ or the peak normalized displacement speed $\max\{S_d(\tau_f\kappa)\}/S_L$ on the unburned gas temperature T_u, computed at various pressures specified in legends and three different equivalence ratios. More specifically, $\max\{S_d(\tau_f\kappa)\}/S_L$ and $\max\{S_c(\tau_f\kappa)\}/S_L$ are larger than unity in all reported cases with the exception of $\max\{S_c(\tau_f\kappa)\}/S_L$ computed at $\Phi=0.7$, $P=10$ bar, and $T_u=900$ K. Thus, the obtained numerical results imply that reduction of differential diffusion effects due to an increase in unburned reactant temperature does not overwhelm enhancement of such effects by pressure, at least if $\Phi\leq0.55$. Therefore, differential diffusion effects are expected to be of importance in engines that burn sufficiently lean hydrogen-air mixtures. This is the main message of the present numerical study.

Please cite this article as: Mousavi SM, Lipatnikov AN, Are differential diffusion effects of importance when burning hydrogen under elevated pressures and temperatures?, International Journal of Hydrogen Energy, https://doi.org/10.1016/j.ijhydene.2023.10.050

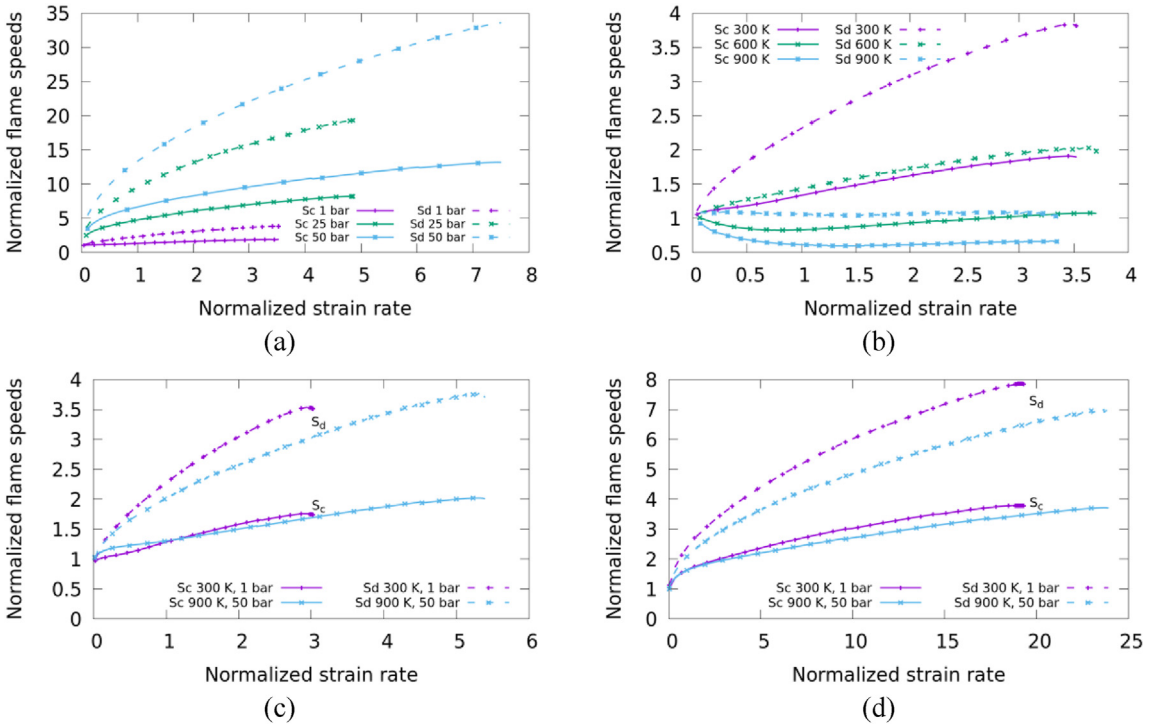

Fig. 4 – Dependencies of normalized displacement speed S_d/S_L (broken lines with symbols) and normalized consumption speed S_c/S_L (solid lines with symbols) on normalized strain rate $\chi\tau_f\kappa$ calculated at (a) $\Phi = 0.55$, $T_u = 300$ K, and various pressures specified in legends, with $\chi = P^*/P$; (b) $\Phi = 0.55$, $P = 1$ atm, and various unburned reactant temperatures specified in legends, with $\chi = (T_u/T_u^*)^2$; (c) $\Phi = 0.55$ and normal (violet lines with pluses) or elevated (blue lines with stars) pressures and temperatures, with $\chi = 1$; and (d) $\Phi = 0.4$ and normal (violet lines with pluses) or elevated (blue lines with stars) pressures and temperatures, with $\chi = 1$. (For interpretation of the references to color in this figure legend, the reader is referred to the Web version of this article.)

This main message holds also when other state-of-the-art chemical mechanisms of hydrogen combustion are used. For instance, Fig. 6 shows that the ratios $\max\{S_c(\tau_f\kappa)\}/S_L$ yielded by three widely recognized mechanisms [88–90] are increased by P and are decreased with increasing T_u, but, nevertheless, are larger than unity in all reported cases. From the quantitative perspective, the ratios $\max\{S_c(\tau_f\kappa)\}/S_L$ yielded by different mechanisms are different, with such differences being more pronounced at higher pressures. The largest reported difference is observed at $T_u = 300$ K and $P = 50$ bar and is about 30 %, cf. curves plotted in violet and green lines in Fig. 6b. Such moderate quantitative differences are not surprising, because the lists of species and, accordingly, the lists of reactions are different for the considered mechanisms. For instance, the mechanism by Curran et al. [89] involves not only OH, but also the excited-state hydroxyl radical OH*, with the latter species being not addressed by the mechanism by Burke et al. [88]. The mechanism by Konnov [90] involves not only OH*, but also two other excited species O* and O_2^*, as well as ozone O_3, with these species being not addressed by the two other mechanisms. Nevertheless, the major reactions in each mechanism are the same (while reaction rate constants are different) and, therefore, quantitative differences between results yielded by these mechanisms are moderate, with qualitative trends being the same. Comparison of capabilities of these mechanisms for predicting speeds of unperturbed or strained laminar flames under elevated pressures and temperatures does not seem to be possible until relevant experimental data are obtained. Accordingly, further discussion of quantitative differences between results yielded by these mechanisms is beyond the scope of the present work.

The influence of temperature and pressure on S_c/S_L or S_d/S_L, observed in Figs. 4–6, is primarily associated with a decrease in Zel'dovich number with increasing T_u and an increase in Ze by P. For instance, the Activation Energy Asymptotic (AEA) theories [55–57] of single-step-chemistry laminar premixed flames predict that magnitude of variations in consumption or displacement speed, caused by differential diffusion effects in stretched flames, is proportional to $Ze(1 - Le)$, where Lewis number $Le = a/D$ is equal to a ratio of molecular heat diffusivity of the mixture to molecular diffusivity of deficient reactant in this mixture. In lean hydrogen-air flames, $D = D_{H_2}$ and $Le < 1$, with Lewis number depending weakly on pressure and temperature. On the contrary, Zel'dovich number is sensitive to both T_u and P. For instance, Fig. 7b and c shows that, for $\Phi = 0.55$ and 0.7, respectively, Ze is decreased with increasing temperature and is increased by pressure. These trends are in line with Fig. 5c-f, which indicate that magnitude of differential diffusion effects is decreased with increasing T_u and is increased by P. However, for the

Please cite this article as: Mousavi SM, Lipatnikov AN, Are differential diffusion effects of importance when burning hydrogen under elevated pressures and temperatures?, International Journal of Hydrogen Energy, https://doi.org/10.1016/j.ijhydene.2023.10.050

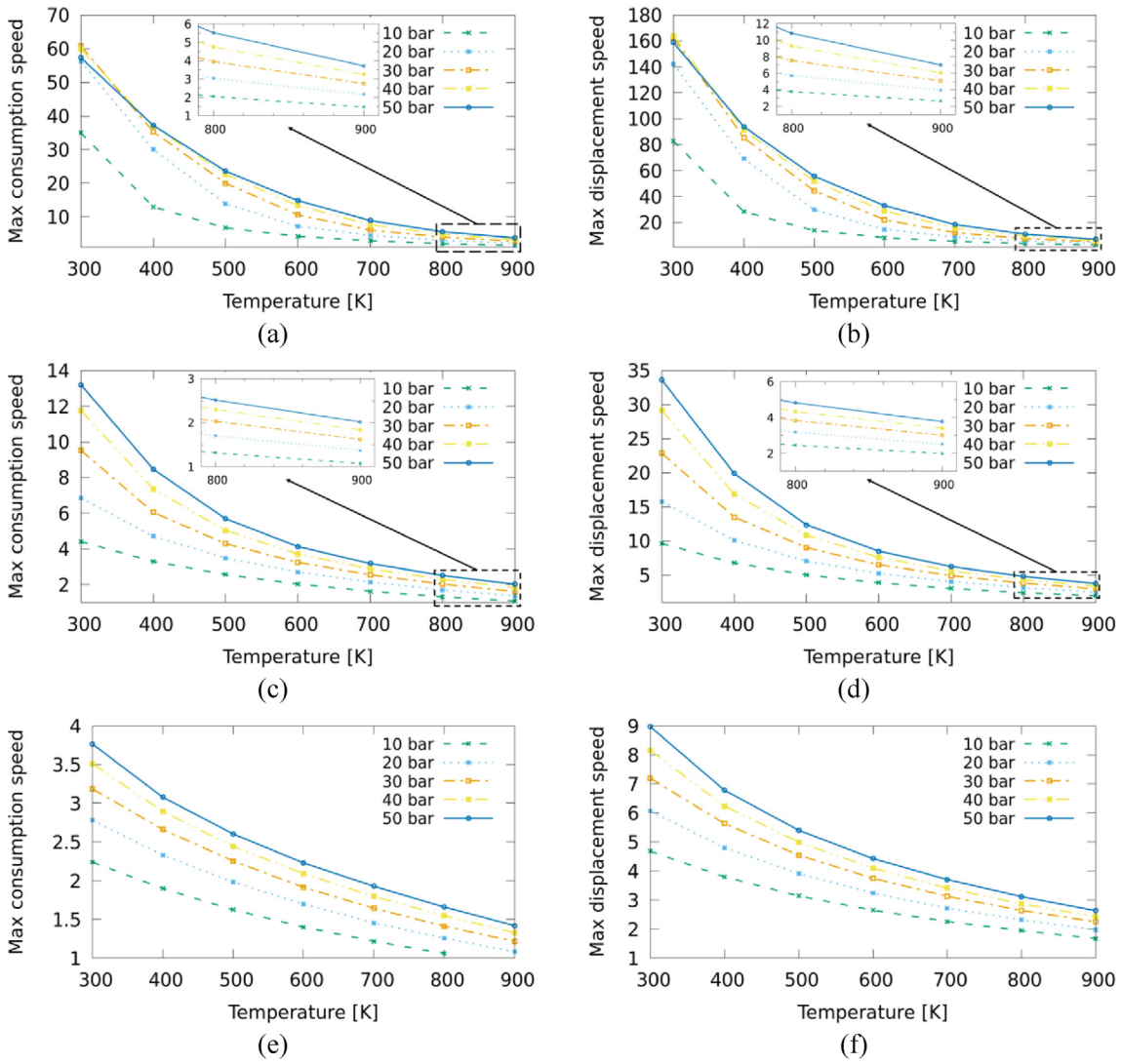

Fig. 5 – Dependencies of (a), (c), and (e) the peak normalized consumption speed $\max\{S_c(\tau_{f^K})\}/S_L$ or (b), (d), and (f) the peak normalized displacement speed $\max\{S_d(\tau_{f^K})\}/S_L$ on the unburned gas temperature T_u, computed at various pressures specified in legends and (a–b) $\Phi = 0.4$, (c–d) $\Phi = 0.55$, or (e–f) $\Phi = 0.7$.

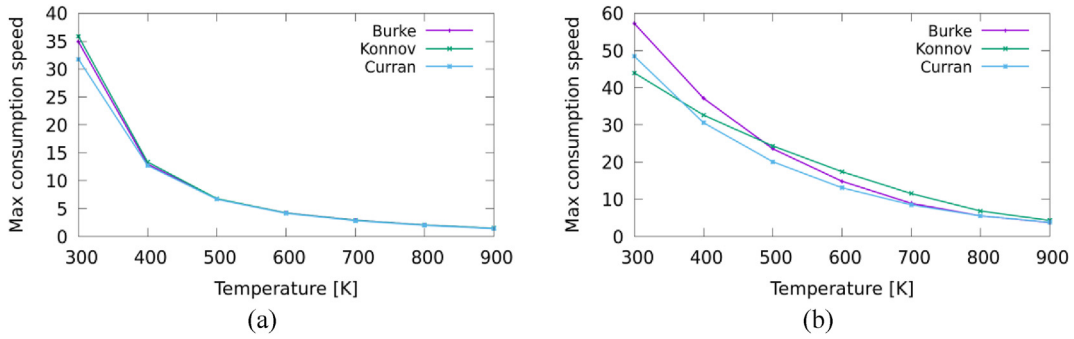

Fig. 6 – Dependencies of the peak normalized consumption speed $\max\{S_c(\tau_{f^K})\}/S_L$ on the unburned gas temperature T_u, computed using chemical mechanisms by Burke et al. [88], Curran et al. [89], and Konnov [90], at (a) $P = 10$ bar and (b) $P = 50$ bar. $\Phi = 0.4$.

leanest mixture ($\Phi = 0.4$), such simple correlations do not hold. On the one hand, Fig. 5a and b indicate that magnitude of differential diffusion effects is decreased with increasing temperature and is increased by pressure, while the latter trend is weakly pronounced at $30 \leq P \leq 50$ bar. On the other hand, dependencies of Ze on T_u and P reported for $\Phi = 0.4$ in Fig. 7a are non-monotonous. For instance, at $T_u = 400$ K, the largest Ze has been computed at $P = 20$ bar, i.e., Ze is increased

Please cite this article as: Mousavi SM, Lipatnikov AN, Are differential diffusion effects of importance when burning hydrogen under elevated pressures and temperatures?, International Journal of Hydrogen Energy, https://doi.org/10.1016/j.ijhydene.2023.10.050

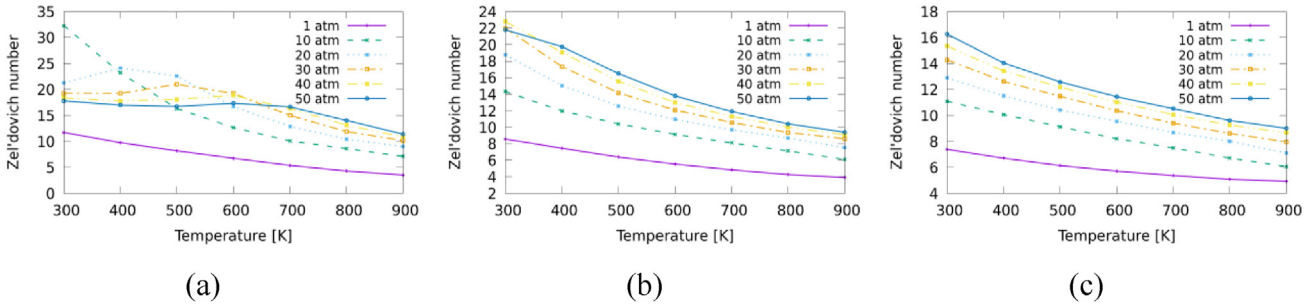

Fig. 7 – Dependencies of Zel'dovich number *Ze* on the unburned gas temperature T_u, computed at various pressures specified in legends. (a) $\Phi = 0.4$, (b) $\Phi = 0.55$, (c) $\Phi = 0.7$.

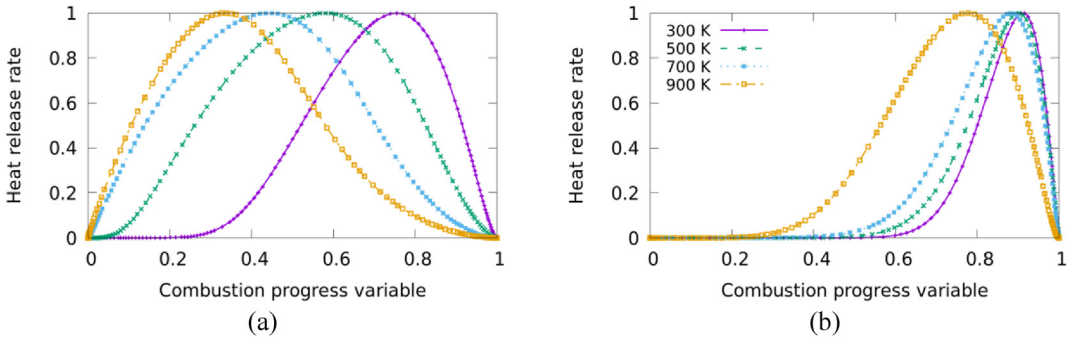

Fig. 8 – Dependencies of normalized heat release rate on temperature-based combustion progress variable $c_T = (T - T_u)/(T_b - T_u)$ obtained from unperturbed laminar premixed flames at various T_u specified in legends and (a) P = 1 bar or (b) P = 50 bar. $\Phi = 0.4$. Heat release rates are normalized using their maximal values, which are different in different flames.

(decreased) with increasing pressure if $P < 20$ bar ($P > 20$ bar, respectively). Moreover, $Ze(T_u)$ either peaks at $T_u = 400$ K if $P = 30$ bar or varies weakly with T_u at $T_u \leq 600$ K if $P = 50$ bar. These qualitative differences between results plotted in Fig. 5a–b and 7a imply that complex chemistry effects play a role also.

In this regard, it is worth recalling that Eqs. (2) and (3) used to evaluate T_a and, subsequently, *Ze* are based on the aforementioned AEA theories of single-step-chemistry laminar premixed flames. In a more general case of complex chemistry, Zel'dovich number characterizes (to the leading order) a ratio of a thickness of a fuel consumption or heat release zone to the entire laminar flame thickness. The lower *Ze*, the wider (relatively) the fuel consumption or heat release zone. Indeed, Fig. 8 shows that, at $\Phi = 0.4$, a relative thickness of heat release zone, i.e., the zone thickness measured in c_T units, is increased by T_u, cf. different curves in Fig. 8a or 8b, but is decreased with increasing pressure, cf. Fig. 8a and b. These complex-chemistry results are in line with Fig. 5a and b, which report data computed at $\Phi = 0.4$.

4. Conclusions

Numerical simulations of lean complex-chemistry hydrogen-air strained laminar flames were performed using three different state-of-the-art chemical mechanisms of hydrogen burning in order to gain insight into eventual importance of differential diffusion effects under elevated pressures and temperatures associated with combustion in future ultra-clean engines. Computed results indicate that differential diffusion effects are more pronounced at higher pressures but are mitigated by mixture preheating, with both trends being mainly attributed to variations in Zel'dovich number with pressure (*Ze* is increased by *P*) and unburned gas temperature (*Ze* is decreased with increasing T_u). Moreover, even at the highest studied $T_u = 900$ K, the extreme consumption speeds obtained from critically strained laminar flames are significantly larger, due to differential diffusion effects, than the counterpart unperturbed laminar flame speeds if the mixture is sufficiently lean (the equivalence ratio $\Phi = 0.55$ or lower) and pressure is sufficiently high ($P \geq 30$ bar). This finding implies that differential diffusion effects can be of substantial importance when burning lean hydrogen-air mixtures in engines and, therefore, calls for development of high-fidelity, physics-based models of the influence of such effects on turbulent burning rate.

Declaration of competing interest

The authors declare that they have no known competing financial interests or personal relationships that could have appeared to influence the work reported in this paper.

Please cite this article as: Mousavi SM, Lipatnikov AN, Are differential diffusion effects of importance when burning hydrogen under elevated pressures and temperatures?, International Journal of Hydrogen Energy, https://doi.org/10.1016/j.ijhydene.2023.10.050

Acknowledgement

This work has been supported by Chalmers Area of Advance *Transport*. Grant number is C 2021-0040.

Nomenclature

Roman symbols

a	molecular heat diffusivity of a mixture
c	combustion progress variable
c_p	heat capacity of a mixture at constant pressure
D	molecular mass diffusivity
$f = \rho_u S_L$	mass burning rate
L	integral length scale of turbulence
Le	Lewis number
P	pressure
r	radial coordinate
$\dot{q}$	heat release rate
S_c	consumption speed, see Eq. (1)
S_d	displacement speed
S_L	unperturbed laminar flame speed
T	temperature
T_a	activation temperature
U_g	inlet flow velocity
U_T	turbulent burning velocity
$\mathbf{u}$	flow velocity vector
u	axial component of flow velocity vector
u'	r.m.s. turbulent velocity
v	radial component of flow velocity vector
X	mole fraction
x	axial coordinate
Ze	Zel'dovich number

Greek symbols

Φ	equivalence ratio
κ	strain rate
ρ	density
τ_f	flame time scale
$\dot{\omega}_F$	fuel consumption rate

Subscripts and superscripts

b	burned
F	fuel
f	flame
u	unburned
ref	reference value
T	temperature or turbulent

Abbreviations

AEA	activation energy asymptotic
CDR	convection-diffusion-reaction
CFD	computational fluid dynamics
DNS	direct numerical simulation
KPP	Kolmogorov-Petrovsky-Piskounov

REFERENCES

[1] Zhu H, Duan J. Research on emission characteristics of hydrogen fuel internal combustion engine based on more detailed mechanism. Int J Hydrogen Energy 2019;44:5592–8.
[2] Yu X, Li G, Du Y, Guo Z, Shang Z, He F, Shen Q, Li D, Li Y. A comparative study on effects of homogeneous or stratified hydrogen on combustion and emissions of a gasoline/hydrogen SI engine. Int J Hydrogen Energy 2019;44:25974–84.
[3] Zhang M, Chang M, Wang J, Huang Z. Flame dynamics analysis of highly hydrogen-enrichment premixed turbulent combustion. Int J Hydrogen Energy 2020;45:1072–83.
[4] Sun H, Yan P, Xu Y. Numerical simulation on hydrogen combustion and flow characteristics of a jet-stabilized combustor. Int J Hydrogen Energy 2020;45:12604–15.
[5] Choubey GDY, Huang W, Yan L, Babazadeh H, Pandey KM. Hydrogen fuel in scramjet engines - a brief review. Int J Hydrogen Energy 2020;45:16799–815.
[6] Öberg S, Odenberger M, Johnsson F. Exploring the competitiveness of hydrogen-fueled gas turbines in future energy systems. Int J Hydrogen Energy 2021;46:624–44.
[7] Babayev R, Andersson A, Dalmau AS, Im HG, Johansson B. Computational characterization of hydrogen direct injection and nonpremixed combustion in a compression-ignition engine. Int J Hydrogen Energy 2021;46:18678–96.
[8] Gao W, Yan Y, Huang L, Zhang W, Shen K. Numerical investigation on combustion characteristics of premixed hydrogen/air in a swirl micro combustor with twisted vanes. Int J Hydrogen Energy 2021;46:40105–19.
[9] Duva BC, Toulson E. Unstretched unburned flame speed and burned gas Markstein length of diluted hydrogen/air mixtures. Int J Hydrogen Energy 2022;47:9030–44.
[10] Yang Z, Wu J, Yun H, Zhang H, Xu J. Diagnosis and control of abnormal combustion of hydrogen internal combustion engine based on the hydrogen injection parameters. Int J Hydrogen Energy 2022;47:15887–95.
[11] Boretti A. High-efficiency internal combustion engine for hybrid hydrogen-electric locomotives. Int J Hydrogen Energy 2023;48:1596–601.
[12] Lai F, Sun B, Wang X, Zhang D, Luo Q, Bao L. Research on the inducing factors and characteristics of knock combustion in a DI hydrogen internal combustion engine in the process of improving performance and thermal efficiency. Int J Hydrogen Energy 2023;48:7488–98.
[13] Shahpouri S, Gordon D, Hayduk C, Rezaei R, Koch CR, Shahbakhti M. Hybrid emission and combustion modeling of hydrogen fueled engines. Int J Hydrogen Energy 2023;48:24037–53.
[14] N PK, Gugulothu SK, Deepanraj B. Numerical analysis of supersonic combustion of hydrogen flow characteristics in scramjet combustor toward the improvement of combustion efficiency. Int J Hydrogen Energy 2023. https://doi.org/10.1016/j.ijhydene.2022.09.135.
[15] Yang Z, Ji C, Yang J, Wang H, Huang X, Wang S. The optimization of leading spark plug location and its influences on combustion and leakage in a hydrogen-fueled Wankel rotary engine. Int J Hydrogen Energy 2023. https://doi.org/10.1016/j.ijhydene.2023.02.099.
[16] Jeelan basha K, Balasubramani S, Sivasankaralingam V. Effect of pre-chamber geometrical parameters and operating conditions on the combustion characteristics of the

Please cite this article as: Mousavi SM, Lipatnikov AN, Are differential diffusion effects of importance when burning hydrogen under elevated pressures and temperatures?, International Journal of Hydrogen Energy, https://doi.org/10.1016/j.ijhydene.2023.10.050

hydrogen-air mixtures in a pre-chamber spark ignition system. Int J Hydrogen Energy 2023. https://doi.org/10.1016/j.ijhydene.2023.03.308.
[17] Anticaglia A, Balduzzi F, Ferrara G, De Luca M, Carpentiero D, Fabbri A, Fazzini L. Feasibility analysis of a direct injection H2 internal combustion engine: numerical assessment and proof-of-concept. Int J Hydrogen Energy 2023. https://doi.org/10.1016/j.ijhydene.2023.04.339.
[18] Zhang X, Ai Q, Wang W. Effects of gas models on radiative heat transfer in the combustion chamber of a hydrogen gas turbine. Int J Hydrogen Energy 2023. https://doi.org/10.1016/j.ijhydene.2023.04.193.
[19] Sorgulu F, Ozturk M, Javani N, Dincer I. Experimental investigation for combustion performance of hydrogen and natural gas fuel blends. Int J Hydrogen Energy 2023. https://doi.org/10.1016/j.ijhydene.2023.05.239.
[20] Aminov RZ, Egorov AN, Schastlivtsev AI. Investigation on combustion efficiency of the hydrogen–oxygen mixture at various pressures and excess oxidizer based on experimental and theoretical studies. Int J Hydrogen Energy 2023. https://doi.org/10.1016/j.ijhydene.2023.06.057.
[21] Acar C, Dincer I. The potential role of hydrogen as a sustainable transportation fuel to combat global warming. Int J Hydrogen Energy 2000;45:3396–406.
[22] Karim GA. Hydrogen as a spark ignition engine fuel. Int J Hydrogen Energy 2003;28:569–77.
[23] Verhelst S, Wallner T. Hydrogen-fueled internal combustion engines. Prog Energy Combust Sci 2009;35:490–527.
[24] Bičáková O, Straka P. Production of hydrogen from renewable resources and its effectiveness. Int J Hydrogen Energy 2012;37:11563–78.
[25] Dincer I, Acar C. A review on potential use of hydrogen in aviation applications. Int J Sustain Aviation 2016;2:74–100.
[26] Yip HL, Srna A, Yuen ACY, Kook S, Taylor RA, Yeoh GH, Medwell PR, Chan QN. A review of hydrogen direct injection for internal combustion engines: towards carbon-free combustion. Appl Sci 2019;9:4842.
[27] Choubey GDY, Huang W, Yan L, Babazadeh H, Pandey KM. Hydrogen fuel in scramjet engines - a brief review. Int J Hydrogen Energy 2020;45:16799–815.
[28] Kovač K, Paranos M, Marciuš D. Hydrogen in energy transition: a review. Int J Hydrogen Energy 2021;46:10016–35.
[29] Stępień Z. A comprehensive overview of hydrogen-fueled internal combustion engines: achievements and future challenges. Energies 2021;14:6504.
[30] Kuznetsov VR, Sabelnikov VA. Turbulence and combustion. Hemisphere; 1990.
[31] Lipatnikov AN, Chomiak J. Molecular transport effects on turbulent flame propagation and structure. Prog Energy Combust Sci 2005;31:1–73.
[32] Lipatnikov AN. Fundamentals of premixed turbulent combustion. CRC Press; 2012.
[33] Karpov VP, Sokolik AS. Ignition limits in turbulent gas mixtures. Proc Acad Sci USSR, Phys Chem 1961;141:866–9.
[34] Karpov VP, Severin ES. Effects of molecular-transport coefficients on the rate of turbulent combustion. Combust Explos Shock Waves 1980;16:41–6.
[35] Wu MS, Kwon A, Driscoll J, Faeth GM. Turbulent premixed hydrogen/air flames at high Reynolds numbers. Combust Sci Technol 1980;73:327–50.
[36] Abdel-Gayed RG, Bradley D, Hamid MN, Lawes M. Lewis number effects on turbulent burning velocity. Proc Combust Inst 1984;20:505–12.
[37] Kido H, Nakahara M. A model of turbulent burning velocity taking the preferential diffusion effect into consideration. JSME Int J 1998;41:666–73.
[38] Daniele S, Jansohn P, Mantzaras J, Boulouchos K. Turbulent flame speed for syngas at gas turbine relevant conditions. Proc Combust Inst 2011;33:2937–44.
[39] Venkateswaran P, Marshall A, Shin DH, Noble D, Seitzman J, Lieuwen T. Measurements and analysis of turbulent consumption speeds of H_2/CO mixtures. Combust Flame 2011;158:1602–14.
[40] Venkateswaran P, Marshall A, Seitzman J, Lieuwen T. Pressure and fuel effects on turbulent consumption speeds of H_2/CO blends. Proc Combust Inst 2013;34:1527–35.
[41] Nguyen MT, Yu DW, Shy SS. General correlations of high pressure turbulent burning velocities with the consideration of Lewis number effect. Proc Combust Inst 2019;37:2391–8.
[42] Yang S, Saha A, Liang W, Wu F, Law CK. Extreme role of preferential diffusion in turbulent flame propagation. Combust Flame 2018;188:498–504.
[43] Zhang M, Wang J, Huang Z. Turbulent flame structure characteristics of hydrogen enriched natural gas with CO_2 dilution. Int J Hydrogen Energy 2020;45:20426–35.
[44] Wang S, Elbaz AM, Arab OZ, Roberts WL. Turbulent flame speed measurement of NH_3/H_2/air and CH_4/air flames and a numerical case study of NO emission in a constant volume combustion chamber. Fuel 2023;332:126152.
[45] Cai X, Fan Q, Bai XS, Wang J, Zhang M, Huang Z, Alden M, Li Z. Turbulent burning velocity and its related statistics of ammonia-hydrogen-air jet flames at high Karlovitz number: effect of differential diffusion. Proc Combust Inst 2023;39:4215–26.
[46] Lipatnikov AN, Chen YR, Shy SS. An experimental study of the influence of Lewis number on turbulent flame speed at different pressures. Proc Combust Inst 2023;39:2339–47.
[47] Aspden AJ, Day MJ, Bell JB. Turbulence-flame interactions in lean premixed hydrogen: transition to the distributed burning regime. J Fluid Mech 2011;680:287–320.
[48] Aspden AJ, Day MJ, Bell JB. Towards the distributed burning regime in turbulent premixed flames. J Fluid Mech 2019;871:1–21.
[49] Lee HC, Dai P, Wan M, Lipatnikov AN. A numerical support of leading point concept. Int J Hydrogen Energy 2022;47:23444–61.
[50] Rieth M, Gruber A, Williams FA, Chen JH. Enhanced burning rates in hydrogen-enriched turbulent premixed flames by diffusion of molecular and atomic hydrogen. Combust Flame 2022;239:111740.
[51] Berger L, Attili A, Pitsch H. Synergistic interactions of thermodiffusive instabilities and turbulence in lean hydrogen flames. Combust Flame 2022;244:112254.
[52] Howarth TL, Hunt EF, Aspden AJ. Thermodiffusively-unstable lean premixed hydrogen flames: phenomenology, empirical modelling, and thermal leading points. Combust Flame 2023;253:112811.
[53] Rieth M, Gruber A, Chen JH. The effect of pressure on lean premixed hydrogen-air flames. Combust Flame 2023;250:112514.

Please cite this article as: Mousavi SM, Lipatnikov AN, Are differential diffusion effects of importance when burning hydrogen under elevated pressures and temperatures?, International Journal of Hydrogen Energy, https://doi.org/10.1016/j.ijhydene.2023.10.050

[54] Berger L, Attili A, Pitsch H. Intrinsic instabilities in premixed hydrogen flames: parametric variation of pressure, equivalence ratio, and temperature. Part 1 - dispersion relations in the linear regime. Combust Flame 2022;240:111935.
[55] YaB Zel'dovich, Barenblatt GI, Librovich VB, Makhviladze GM. The mathematical theory of combustion and explosions. Consultants Bureau; 1985.
[56] Clavin P. Dynamical behavior of premixed flame fronts in laminar and turbulent flows. Prog Energy Combust Sci 1985;11:1–59.
[57] Matalon M. Flame dynamics. Proc Combust Inst 2009;32:57–82.
[58] Karpov V, Lipatnikov A, Zimont V. A test of an engineering model of premixed turbulent combustion. Proc Combust Inst 1996;26:249–57.
[59] Verma S, Monnier F, Lipatnikov AN. Validation of leading point concept in RANS simulations of highly turbulent lean syngas-air flames with well-pronounced diffusional-thermal effects. Int J Hydrogen Energy 2021;46:9222–33.
[60] Ebert U, van Saarloos W. Front propagation into unstable states: universal algebraic convergence towards uniformly translating pulled fronts. Physica D 2000;146:1–99.
[61] van Saarloos W. Front propagation into unstable states. Phys Rep 2003;386:29–222.
[62] Fisher RA. The wave of advance of advantageous genes. Ann. Eugenics 1937;7:355–69.
[63] Kolmogorov AN, Petrovsky I, Piskounov N. A study of the diffusion equation with a source term and its application to a biological problem. Bjull MGU A 1937;1(6):1–26 (English translation in Pelcé P, editor. Dynamics of curved fronts. Academic Press; 1988. pp. 105–130).
[64] Murray JD. Lectures on nonlinear-differential-equation models in biology. Clarendon Press; 1977.
[65] Murray JD. Mathematical biology 1. An introduction. 3rd ed. Springer; 2002.
[66] Bray KNC, Libby PA. Interaction effects in turbulent premixed flames. Phys Fluids 1976;19:1687–701.
[67] Hakberg B, Gosman AD. Analytical determination of turbulent flame speed from combustion models. Proc Combust Inst 1984;20:225–32.
[68] Libby PA. Theory of normal premixed turbulent flames revisited. Prog Energy Combust Sci 1985;11:83–96.
[69] Bray KNC. Studies of the turbulent burning velocity. Proc R Soc London, A 1990;431:315–35.
[70] Catlin CA, Lindstedt RP. Premixed turbulent burning velocities derived from mixing controlled reaction models with cold front quenching. Combust Flame 1991;85:427–39.
[71] Duclos J, Veynante D, Poinsot T. A comparison of flamelet models for premixed turbulent combustion. Combust Flame 1993;95:101–18.
[72] Choi CR, Huh KY. Development of a coherent flamelet model for spark-ignited turbulent premixed flame in a closed vessel. Combust Flame 1998;114:336–48.
[73] Kolla H, Rogerson JW, Chakraborty N, Swaminathan N. Scalar dissipation rate modeling and its validation. Combust Sci Technol 2009;181:518–35.
[74] Kolla H, Rogerson JW, Swaminathan N. Validation of a turbulent flame speed model across combustion regimes. Combust Sci Technol 2010;182:284–308.
[75] Zhang W, Wang J, Yu Q, Jin W, Zhang M, Huang Z. Investigation of the fuel effects on burning velocity and flame structure of turbulent premixed flames based on leading points concept. Combust Sci Technol 2018;190:1354–76.
[76] Sabelnikov VA, Lipatnikov AN. Transition from pulled to pushed premixed turbulent flames due to countergradient transport. Combust Theor Model 2013;17:1154–75.
[77] Sabelnikov VA, Lipatnikov AN. Transition from pulled to pushed fronts in premixed turbulent combustion: theoretical and numerical study. Combust Flame 2015;162:2893–903.
[78] Kha KQN, Robin V, Mura A, Champion M. Implications of laminar flame finite thickness on the structure of turbulent premixed flames. J Fluid Mech 2016;787:116–47.
[79] Somappa S, Acharia V, Lieuwen T. Finite flame thickness effects on KPP turbulent burning velocities. Phys Rev E 2022;106:55107.
[80] Kim SH. Leading points and heat release effects in turbulent premixed flames. Proc Combust Inst 2017;36:2017–24.
[81] Dave HL, Mohan A, Chaudhuri S. Genesis and evolution of premixed flames in turbulence. Combust Flame 2018;196:386–99.
[82] Lipatnikov AN, Chakraborty N, Sabelnikov VA. Transport equations for reaction rate in laminar and turbulent premixed flames characterized by non-unity Lewis number. Int J Hydrogen Energy 2018;43:21060–9.
[83] Lee HC, Dai P, Wan M, Lipatnikov AN. Influence of molecular transport on burning rate and conditioned species concentrations in highly turbulent premixed flames. J Fluid Mech 2021;928:A5.
[84] Lee HC, Dai P, Wan M, Lipatnikov AN. Displacement speed, flame surface density, and burning rate in highly turbulent premixed flames characterized by low Lewis numbers. J Fluid Mech 2023;961:A21.
[85] Zimont VL, Lipatnikov AN. A numerical model of premixed turbulent combustion of gases. Chem Phys Reports 1995;14:993–1025.
[86] Lee HC, Abdelsamie A, Dai P, Wan M, Lipatnikov AN. Influence of equivalence ratio on turbulent burning velocity and extreme fuel consumption rate in lean hydrogen-air turbulent flames. Fuel 2022;327:124969.
[87] Dixon-Lewis G. Structure of laminar flames. Proc Combust Inst 1990;23:305–24.
[88] Burke MP, Chaos M, Ju Y, Dryer FL, Klippenstein SJ. Comprehensive H_2/O_2 kinetic model for high-pressure combustion. Int J Chem Kinet 2012;44:444–74.
[89] Kéromnès A, Metcalfe WK, Heufer KA, Donohoe N, Das AK, Sung CJ, Herzler J, Naumann C, Griebel P, Mathieu O, Krejci MC, Petersen EL, Pitz WJ, Curran HJ. An experimental and detailed chemical kinetic modeling study of hydrogen and syngas mixture oxidation at elevated pressures. Combust Flame 2013;160:995–1011.
[90] Konnov AA. Yet another kinetic mechanism for hydrogen combustion. Combust Flame 2019;203:14–22.
[91] Goodwin D, Malaya N, Moffat H, Speth R. Cantera: an object-oriented software toolkit for chemical kinetics, thermodynamics, and transport processes. Pasadena, CA: Caltech; 2009.
[92] Law CK, Sung CJ. Structure, aerodynamics, and geometry of premixed flamelets. Prog Energy Combust Sci 2000;26:459–505.

Please cite this article as: Mousavi SM, Lipatnikov AN, Are differential diffusion effects of importance when burning hydrogen under elevated pressures and temperatures?, International Journal of Hydrogen Energy, https://doi.org/10.1016/j.ijhydene.2023.10.050